

Chapter 5

Formation of Supramolecular Polymers from Homoditopic Molecules Containing Secondary Ammonium Ion and Crown Ether Moieties

5.1. Introduction

Chemists are extending the concept of self-organizing non-covalent interactions into the field of material science to control and engineer linear and network supramolecular polymers.¹ Such interactions permit reversibility in the polymeric materials at the molecular level, affording thermodynamically controlled suprastructures.²⁻⁹ This is advantageous from the view of producing polymers with potential for commercial use, since kinetically induced defects in conventional covalently bonded polymers are irreversible.

It has been shown that strong associations between self-organizing building blocks promote the construction of well-defined supramolecular polymeric materials with properties comparable to covalent polymers.¹⁰⁻¹³ This prompted us to utilize a simple system with dibenzylammonium hexafluorophosphate and dibenzo-24-crown-8 (DB24C8) units, between which the association constant is desirably high ($K_a=2.7 \times 10^4 \text{ M}^{-1}$ in chloroform-*d* at 25°C).^{14,15} Association of homoditopic molecules containing such complementary units spontaneously leads to reversible chain extension in 1:1 stoichiometric solutions, forming linear supramolecular polymers based on pseudorotaxane formation as we describe in this chapter.

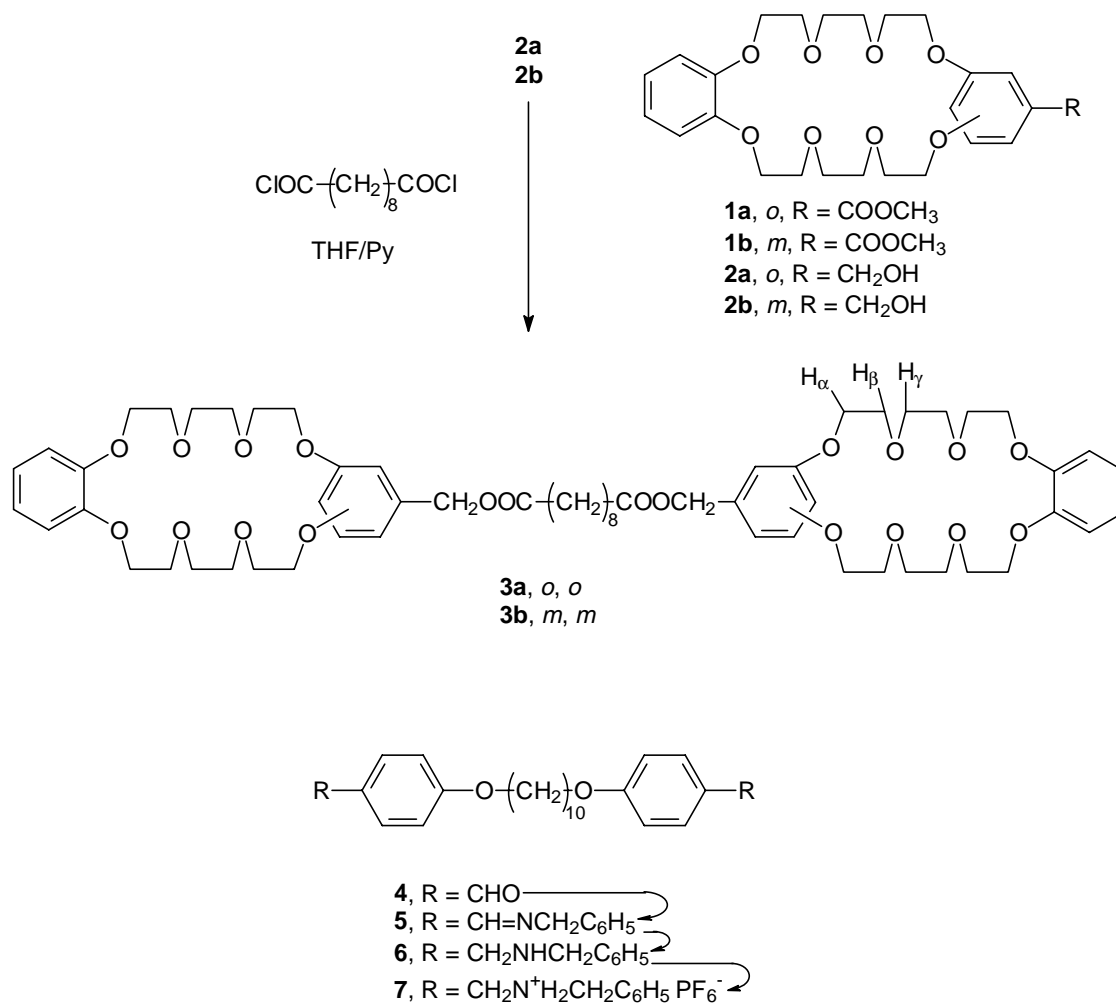


Figure 5.1. Synthesis of **3a**, **3b**, and **7**.

5.2. Results and Discussion

5.2.1. Synthesis

The synthetic methodologies employed for the homoditopic molecules are depicted in Figure 5.1 and the constructions of self-organized supramolecules are illustrated in Figure 5.2. The ester group of **1** was reduced to the primary alcohol group (**2**), which was then esterified with sebacoyl chloride in the presence of pyridine to afford the bis-crown homoditopic molecule **3**. In the ¹H NMR spectrum of **3** the signal for the benzyl protons was shifted downfield with respect to that of **2** due to the formation of the ester group. A typical procedure involving continuous removal of water to shift the equilibrium to the right was used for the synthesis of **5** from benzylamine and the

corresponding dialdehyde **4**. The ^1H NMR spectrum of **5** revealed a characteristic singlet corresponding to the imine proton at 8.31 ppm. The electron withdrawing nature of adjacent C=N linkage gives rise to the significant downfield chemical signal shift observed for this proton. Additional evidence for the Schiff base **5** formation came from a new signal emerging at 4.79 ppm for the benzyl proton. The Schiff base was immediately reduced in a mild condition with sodium borohydride to give the corresponding amine **6**. Two sharp singlets observed for the benzyl protons at 3.75 and 3.80 ppm and the disappearance of the imine signal in the ^1H NMR spectrum of **6** assured the successful reduction reaction. This imine was finally acidified and followed by an ion exchange reaction to obtain the homoditopic ammonium salt **7**, which showed improved solubility in organic solvents such as in acetone and acetonitrile with PF_6^- counter ions compared to Cl^- .

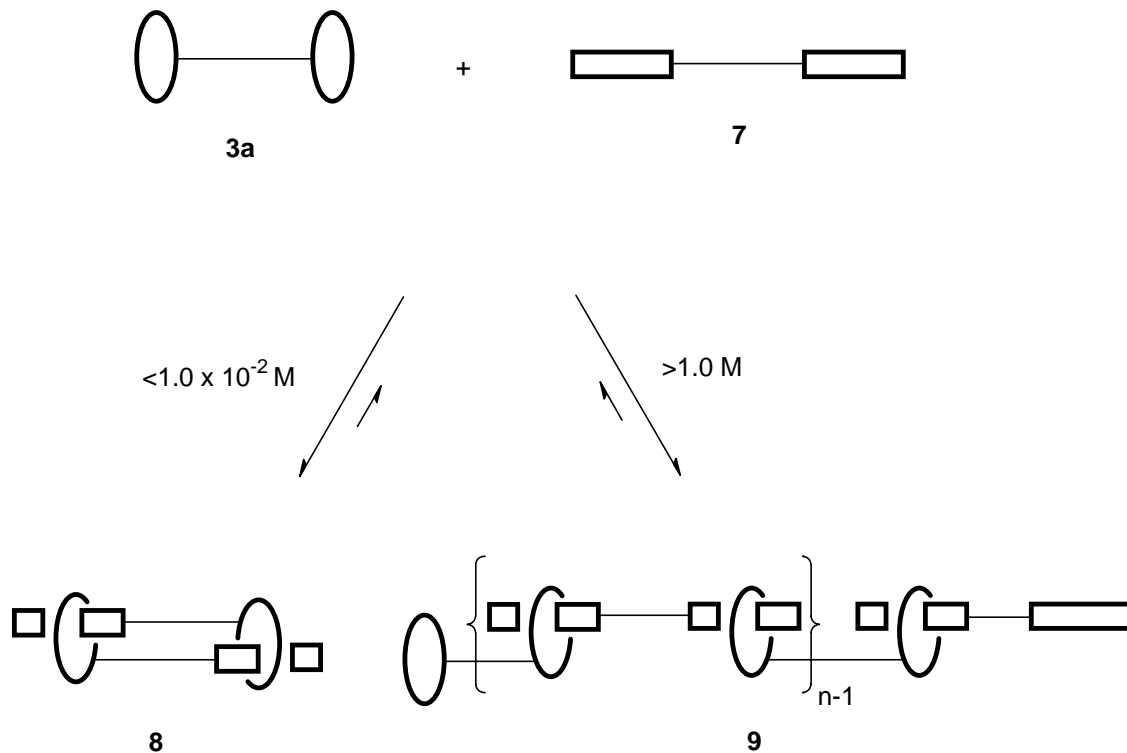


Figure 5.2. Illustration of the constructions of the supramolecules **8** and **9** from **3a** and **7**.

To test the complexation behavior of **7** with dibenzo-24-crown-8, a solution of the two (10 mM/ 20 mM, **7**/DB24C8) in acetone- d_6 /chloroform- d (1/1, v/v) was

investigated with ^1H NMR spectroscopy. Based on the assumption that the complexation at the ammonium salt moieties of **7** are independent of each other, the association constant (K_a) for the pseudorotaxane formation was determined to be $3.5 \times 10^{-2} \text{ M}^{-1}$ at 22°C by single point measurements. This spectroscopic observation led us to proceed to construct supramolecular aggregates, namely linear arrays, using the two complementary homoditopic molecules of **3a** and **7**.

5.2.2. Complexation studies in solution

The ^1H NMR spectrum of an equimolar solution of **3a** and **7** in acetone- d_6 /chloroform- d (1/1, v/v) showed three sets of signals for the benzylic protons of **7** at 22°C (*e.g.*, Figure 5.3d). Two of these can be attributed to the signals for complexed **7** while the other set corresponds to the signals for uncomplexed **7** based on the argument of slow exchange on the ^1H NMR time scale. The two sets of signals for complexed **7** arise from two different pseudorotaxane structures, the cyclic dimer **8** and linear chain **9**. The chemical shifts of the signals for complexed **7** in the 1:1 cyclic dimer **8** are unique from those in the linearly linked chain **9** due to the discrete geometry adopted by **8**. To assign the two sets of signals properly, a series of $1.0 \times 10^{-2} \text{ M}$ solutions of **7** were prepared using non-stoichiometric amounts of **3a** (from $2.0 \times 10^{-2} \text{ M}$ to $8.0 \times 10^{-2} \text{ M}$) and the ^1H NMR spectra were recorded at 22°C (Figure 5.4). Increasing the concentration of **3a** with respect to **7** shifts the complexation equilibrium toward the formation of the 1:2 complex **7:(3a)₂**, emulating the environment of the benzylic methylene units in **9**. Since the signals at 4.53 and 4.63 ppm become more intense, while the signals at 4.45 and 4.74 ppm become less intense, as the solution is more concentrated in **3a**, the former (inner) signals correspond to the benzylic protons of complexed **7** in the linearly linked chain **9** and the latter (outer) signals to those in the 1:1 cyclic dimer **8**.

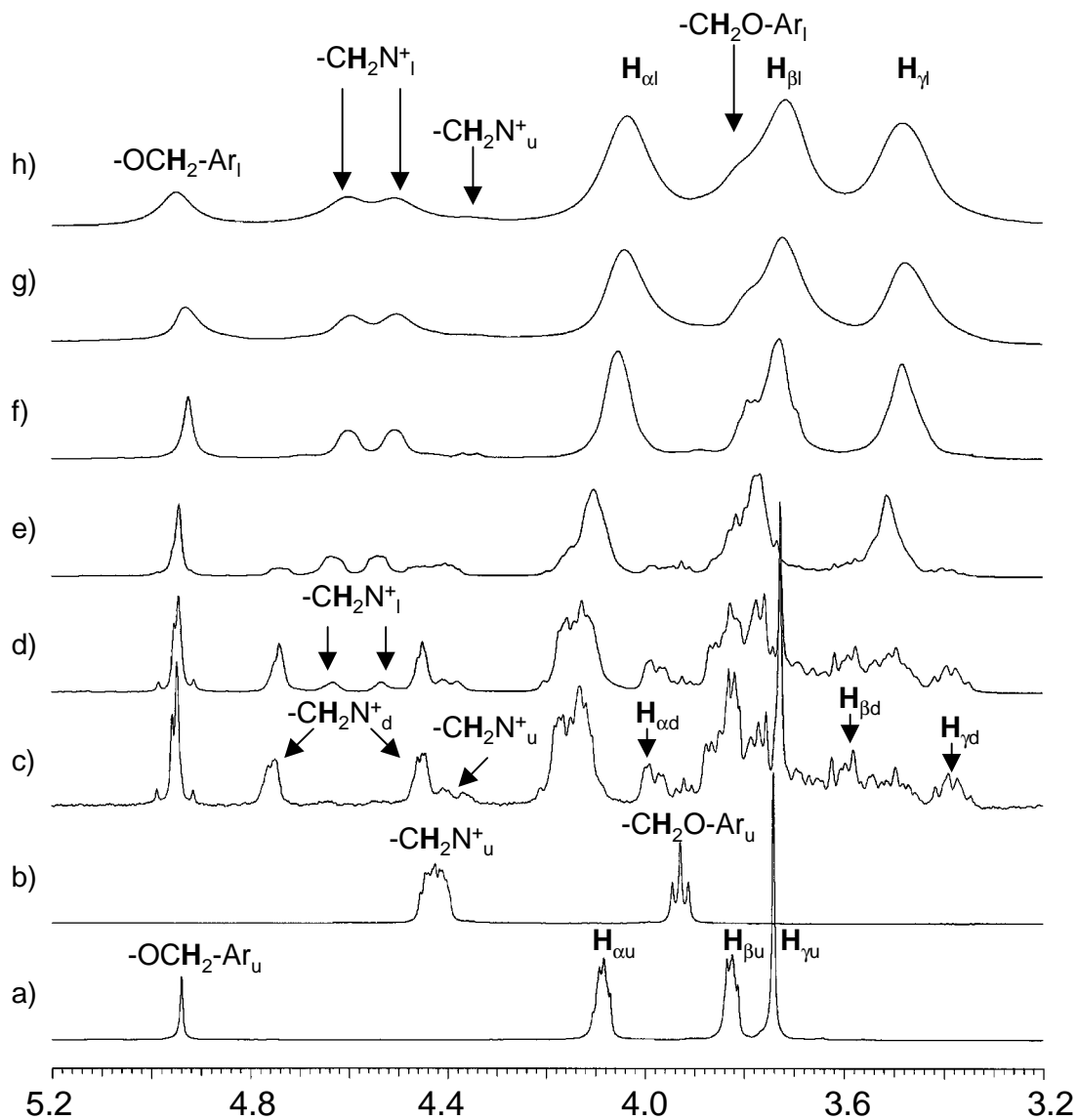


Figure 5.3. The stacked ^1H NMR spectra of solutions of **3a** and **7** at a) $1.0 \times 10^{-2}/0$, b) $0/1.0 \times 10^{-2}$, and c) 1.0×10^{-3} , d) 1.0×10^{-2} , e) 0.10, f) 0.50, g) 1.0, and h) 2.0 M equimolar solutions (400 MHz, acetone- d_6 /chloroform- d (1/1, v/v), 22°C). The three sets of signals are for uncomplexed **3a** and **7** (u), **8** (d), and **9** (I).

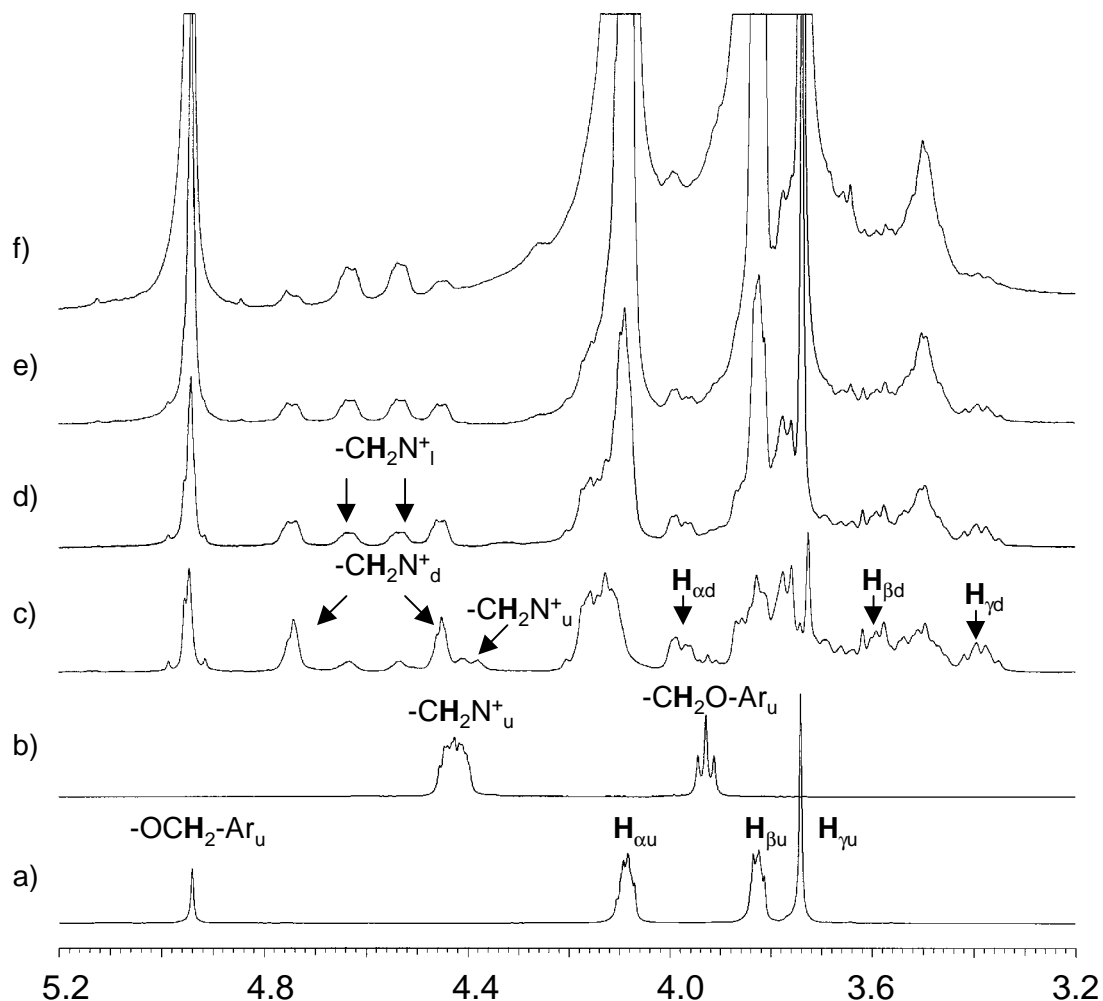


Figure 5.4. The stacked ^1H NMR spectra of solutions of **3a** and **7** at a) $1.0 \times 10^{-2}/0$, b) $0/1.0 \times 10^{-2}$, c) $1.0 \times 10^{-2}/1.0 \times 10^{-2}$, d) $2.0 \times 10^{-2}/1.0 \times 10^{-2}$, e) $4.0 \times 10^{-2}/1.0 \times 10^{-2}$, f) $8.0 \times 10^{-2} \text{ M}/1.0 \times 10^{-2} \text{ M}$ (400 MHz, acetone- d_6 /chloroform- d (1/1, v/v), 22°C). The three sets of signals are for uncomplexed **3a** and **7** (u), **8** (d), and **9** (l).

The ^1H NMR spectra (Figure 5.3) recorded at different concentrations of equimolar solutions of **3a** and **7** in acetone- d_6 /chloroform- d (1/1, v/v) at 22°C revealed that both the ratio of **8:9** and the extent of aggregation in **9** are concentration dependent. At lower equimolar concentrations ($<1.0 \times 10^{-2} \text{ M}$) the ^1H NMR spectra revealed more intense signals for complexed **7** in the cyclic dimer **8** than in the linear chain **9**. For instance, 72 and 66% of each homoditopic molecule are consumed to form the 1:1 cyclic dimer **8** in 1.0×10^{-3} and $1.0 \times 10^{-2} \text{ M}$ equimolar solutions at 22°C , respectively (Table 1). The NOESY spectrum of the $1.0 \times 10^{-3} \text{ M}$ equimolar solution recorded at 22°C showed a

through-space interaction between the protons of the methylene units of corresponding homoditopic molecules **3a** and **7**, indicating the presence of the 1:1 cyclic dimer **8**. In contrast, at the highest equimolar concentration we examined (2.0 M), the signals for the 1:1 cyclic dimer are no longer observed (Figure 5.3h), indicating its absence. Since the concentrations of the end-groups in the supramolecular polymers **9** are readily determined by integrating the signal for uncomplexed **7** in the corresponding ^1H NMR spectra, one can estimate the average molecular weight of the linearly linked chain **9** at a given concentration (Table 1). The ratio of the percentage of ammonium ion units in **9** to the percentage of uncomplexed ammonium ion units is equal to $2n$. Thus, solving this equation yields $n = (100 - \% \text{ of ammonium ion units in } \mathbf{8})/2(\% \text{ uncomplexed ammonium ion units})$. From the n value and the repeat unit mass (1980 Da) the number average molar mass, M_n , of **9** was calculated. For instance, in the 1.0 M equimolar solution $M_n=15$ kDa ($n=7.5$). The 2.0 M equimolar solution gives an even higher molecular weight of 18 kDa ($n=9.1$). Substantially broadened signals in Figures 5.3g and 5.3h strongly support the formation of large supramolecular polymers **9** in solution. The average molecular weight of **9** was calculated assuming the absence of the cyclic oligomers such as 2:2 and 3:3 complexes. It is noteworthy that linear polymerization is highly favored over cyclization at high solution concentrations,^{16,17} e.g., 1.0 M. Therefore, the assumption of the absence of the oligomeric cyclic complexes is valid in the more concentrated solutions. The percentage of ammonium ion units in **9** is equal to 100 minus the percentage of ammonium ion units in **8**.

Table 5.1. Analyses of percentages of ammonium ion moieties in dimer **8** and supramolecular polymer **9**, and the average number of repeat units, n , in **9**.^a

equimolar conc. (M)	% in 8 at +22/-40°C	% uncomp. at +22/-40°C	n^c at +22/-40°C	M_n^d at +22/-40°C (kDa)
2.0	0/- ^b	5.5/- ^b	9.1/- ^b	18/- ^b
1.0	3.4/- ^b	6.4/- ^b	7.5/- ^b	15/- ^b
0.50	12/15	7.9/5.1	5.6/8.3	11/16
0.10	23/27	20/5.4	1.9/6.8	3.8/13
1.0x10 ⁻²	66/81	16/4.3	1.1/2.2	2.2/4.4
1.0x10 ⁻³	72/94	20/2.3	0.70/1.3	1.4/2.6

a) Calculated from the ¹H NMR spectra of equimolar solutions (acetone-*d*₆/chloroform-*d*, 1/1, v/v) of **3a** and **7** at various concentrations and temperatures.

b) The ¹H NMR spectra of the 2.0 and 1.0 M equimolar solutions recorded at lower temperatures exhibited severe signal broadening, preventing accurate signal integration.

c) n was determined by solving the expression; $n = (100 - \% \text{ of ammonium ion units in } \mathbf{8}) / 2(\% \text{ uncomplexed ammonium ion units})$.

d) The number average molecular weight (M_n) of the aggregate was calculated using the following equation; $M_n = n \times 1980 \text{ Da}$ (repeat unit mass).

The plot of reduced viscosity versus concentration of equimolar solutions of **3a** and **7** in acetone-*d*₆/chloroform-*d* (1/1, v/v) at 22°C is non-linear (Figure 5.5b), reflecting the increasing size of the supramolecular polymer **9** with concentration as shown by the ¹H NMR data. In fact, the viscosities of 1.0 and 2.0 M equimolar solutions were too high to measure by this method. On the other hand, a completely different solution viscosity profile was observed for equimolar solutions of **3b**, a constitutional isomer of **3a**, and **7** (Figure 5.5a). It should be noted that the ¹H NMR spectrum of an equimolar solution of **1b** and dibenzylammonium hexafluorophosphate in the same solvent system displayed no sign of complexation. The ¹H NMR spectrum of a 1:1 stoichiometric solution of **1b** and dibenzylammonium hexafluorophosphate at 1.0 x 10⁻² M in acetone-*d*₆/chloroform-*d* (1/1, v/v) did not show extra sets of signals due to slow exchange or changes in the chemical shifts due to fast exchange. The *m*-phenylene linkage in the crown moieties of **1b** prevents pseudorotaxane formation in solution. A straight line with low slope in Figure 5.5a is consistent with the ¹H NMR observation that there is no complexation between **3b** and **7** in solution. It also indicates that the ionic strength per se has a negligible effect on viscosity under these experimental conditions. Therefore, the sharp increase in viscosity

at higher concentrations in Figure 5.5b is reflective of the aggregation between **3a** and **7**, producing structures of large hydrodynamic volume, *i.e.*, **9**.

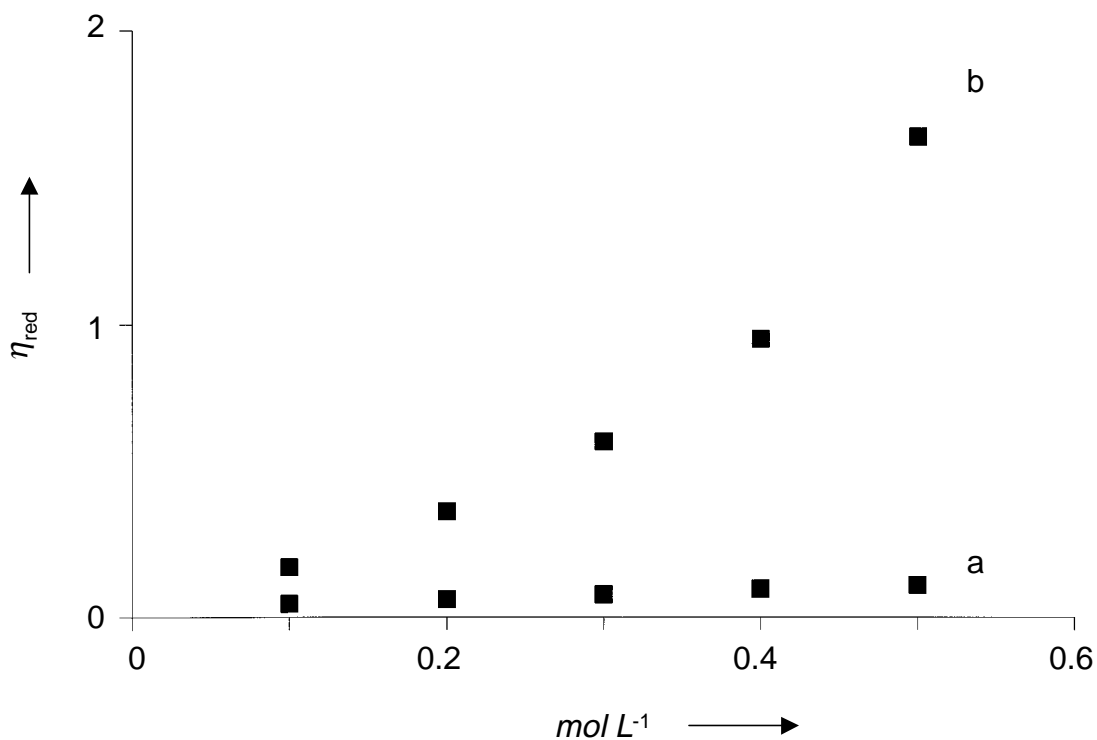


Figure 5.5. Reduced viscosity as a function of concentration in acetone/chloroform (1/1, v/v) at 22°C for a) **3b** and **7** and b) **3a** and **7**.

5.2.3. Characterization of linear arrays in the solid state

Yellow-orange solid samples prepared by using a freeze-drying technique in which the 1.0×10^{-2} , 0.10, and 0.50 M equimolar solutions of **3a** and **7** in acetone/chloroform (1/1, v/v) were frozen at -93°C with an acetone-ethanol/liquid nitrogen bath and the solvents were removed under high vacuum. The samples were then analyzed by differential scanning calorimetry (DSC) (Figure 5.6). To eliminate sample history, the freeze-dried samples were initially heated to 100°C and cooled to 30°C at the rate of 10°C min⁻¹. They were then heated at 10°C min⁻¹ and the DSC thermograms were recorded. M_n of the supramolecular polymer **9** and the abundance of the 1:1 cyclic dimer **8** in each sample were estimated from low temperature ¹H NMR spectra (Table 1). It

should be noted that the ^1H NMR spectra of equimolar solutions of **3a** and **7** at 1.0×10^{-2} , 0.10, and 0.50 M in acetone- d_6 /chloroform- d (1/1, v/v) were essentially unchanged from -40 to -60°C (below this temperature the ^1H NMR spectra of the solutions were unable to be recorded due to partial freezing of the solvents). Thus, M_n 's of the freeze-dried (-93°C) samples were estimated by simple integration of relevant signals of the spectra recorded at -40°C . The DSC thermograms for the 0.10 and 0.50 M materials (Figure 5.6a shows the DSC trace of the 0.50 M sample) were entirely different from those observed for the pure homoditopic molecules **3a** and **7**, which were crystalline in nature. As a result of self-organization, amorphous polymers **9** with T_g 's above 50°C were formed for the 0.10 and 0.50 M samples (57 and 59°C , respectively). From end-group analysis the 0.10 and 0.50 M materials contained supramolecular polymers **9** of $M_n=13$ kDa and 16 kDa, respectively (Table 1). The polymers became rubber-like materials above T_g and thus they may be processable. In the case of the 1.0×10^{-2} M sample (81% cyclic dimer **8**, Table 1), a high degree of crystallinity was observed by optical microscopy. Indeed, the DSC trace obtained for this sample displayed no T_g up to 140°C (Figure 5.6b). Presumably, compactness and the semi-rigid nature of **8** allow stable packing in the crystal lattice.¹⁸ It is noteworthy that the thermal decomposition of the secondary ammonium salt moieties of **7** gives HPF_6 and the corresponding secondary amine is believed to attack the ester linkage of **3a** to afford a polyamide and alcohol **2a**.

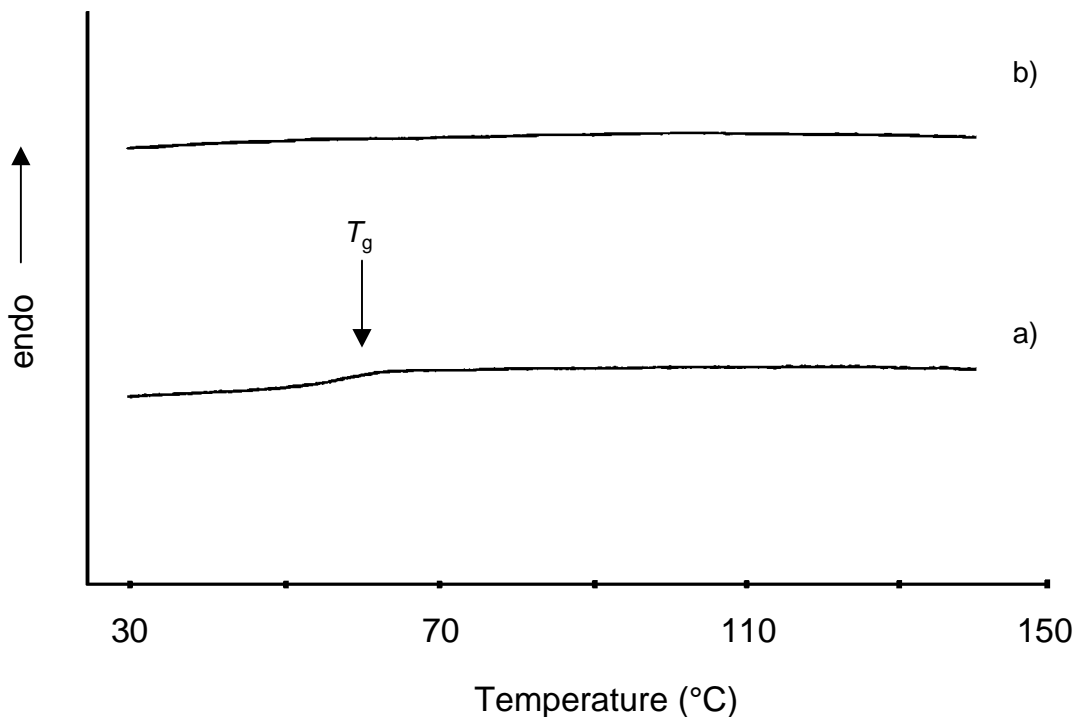


Figure 5.6. DSC traces of a) the 0.50 M sample and b) 1.0×10^{-2} M sample (2nd heating at $10^\circ\text{C}/\text{min}$).

Flexible, creasible, amorphous, and transparent films can be cast from 1:1 stoichiometric solutions of **3a** and **7**. Such properties can only result from entanglement of linearly connected macro-sized aggregates. Similarly, since a polymer structure of high molecular weight is necessary for fiber formation, the scanning electron microscope images (Figures 5.7a and 5.7b) of a rod-like fiber with regular diameter of $10 \mu\text{m}$ drawn from a concentrated equimolar solution of **3a** and **7** in acetone/chloroform (1/1, v/v) indicate a high degree of the linear chain extension in **9**. It must be noted that these fibers were formed in a manner analogous to that used for covalently bonded macromolecules (dry spinning¹⁹) and not by gelation in a poor solvent, which has also yielded fibers via self-organization.²⁰⁻²²

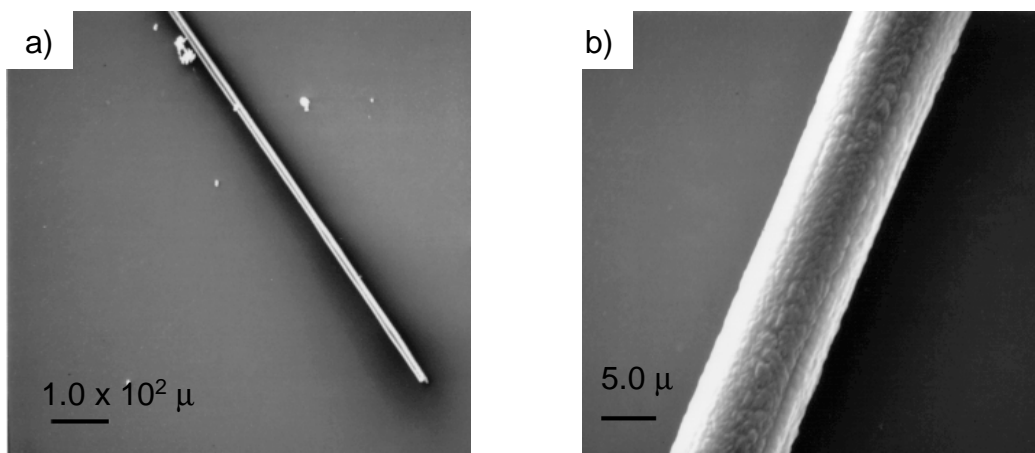


Figure 5.7. Longitudinal views of scanning electron micrographs of a fiber pulled from a concentrated acetone/chloroform (1/1, v/v) equimolar solution of **3a** and **7** (>2.0 M) a) low resolution b) high resolution.

5.3. Conclusions

In summary, the 1:1 cyclic dimer complex **8** is preferentially formed in dilute equimolar solutions (<1.0 x 10⁻² M), while linear chain extension to **9** is observed almost exclusively in concentrated equimolar solutions (>1.0 M). The solution behavior of the self-organized supramolecules **9** was characteristic of large aggregates as demonstrated by the viscosity experiments. The solid state samples prepared by freeze-drying 0.10 and 0.50 M equimolar solutions showed that the supramolecules **9** are amorphous polymers. The preparation of films and fibers corroborates the polymeric nature of the self-organized suprastructures **9**.

5.4. Experimental

Pyridine and was stirred with CaH₂ overnight and distilled prior to the polymerization reactions. THF was distilled from Na and benzophenone. All other solvents were used as received. Melting points were taken on a Mel-Temp II melting point apparatus and are uncorrected. The 400 MHz ¹H NMR spectra were recorded on a Varian Unity with tetramethylsilane (TMS) as an internal standard. The following abbreviations are used to denote splitting patterns: s (singlet), d (doublet), t (triplet), and m (multiplet). Differential scanning calorimetry (DSC) was performed on a Perkin-Elmer Series-4 calorimeter under a nitrogen purge using indium as the calibration standard.

Scanning electron microscopy (SEM) was performed on a Philips 420T. The copper substrate was sputtered with gold after sample deposition and before exposure to the electron beam. Elemental analyses were obtained from Atlantic Microlab, Norcross, GA. Mass spectra were provided by the Washington University Mass Spectrometry Resource, an NIH Research Resource (Grant No. P41RR0954). The syntheses of **1a**, **1b**, **2a**, and **2b** are described in details in chapter 2. **4** was prepared by the procedure reported in the literature.^{23,24}

General procedure for 3a and 3b. To a 100 mL three necked round bottom flask equipped with a magnetic stirrer, a condenser, and a N₂ inlet were added sebacoyl chloride (1.00 equiv.), pyridine (2.20 equiv.), and anhydrous THF. To this was added a solution of **2** (2.00 equiv.) in THF via syringe and the mixture was stirred at 40°C for 12 h. The salt was filtered and the filtrate was concentrated to give an off-white solid, which was recrystallized from EtOH.

3a. 80% yield, mp 120–122°C. ¹H NMR (400 MHz, chloroform-*d*, 22°C): δ=1.23-1.27 (8H, m), 1.57 (4H, m), 2.31 (4H, t, *J* = 8.0 Hz) 3.83 (8H, s), 3.91 (8H, t, *J* = 4.0 Hz), 5.00 (4H, s), 6.82 (1H, d, *J* = 8.0 Hz), and 6.85-6.91 (6H, m). LRFAB: *m/z* = 1123.2 [*M*+H]⁺. HRFAB: calcd for [*M*]⁺ C₆₀H₈₂O₂₀ 1122.5399, found 1122.5374. Anal. Calcd for C₆₀H₈₂O₂₀: C, 64.14; H, 7.36, found: C, 64.10; H, 7.40.

3b. 90% yield, mp 78-80°C. ¹H NMR (400 MHz, chloroform-*d*, 22°C): δ=1.25-1.29 (8H, m), 1.63 (4H, m), 2.33(4H, t, *J* = 8.0 Hz), 3.72 (8H, s), 3.82 (4H, t, *J* = 4.0 Hz), 3.85 (4H, t, *J* = 4.0 Hz), 4.15 (8H, t, *J* = 4.0 Hz), 5.00 (4H, s), 6.48 (2H, d, *J* = 1.6 Hz), 6.66 (1H, t, *J* = 1.6 Hz), and 6.87-6.92 (4H, m). LRFAB: *m/z* = 1123.2 [*M*+H]⁺. HRFAB: calcd for [*M*]⁺ C₆₀H₈₂O₂₀ 1122.5399, found 1122.5372. Anal. Calcd for C₆₀H₈₂O₂₀: C, 64.14; H, 7.36, found: C, 64.06; H, 7.29.

5. To a two necked round bottom flask equipped with a Dean-Stark trap, a condenser, and a N₂ inlet were added **4** (3.54 g, 9.25 mmol) and toluene (125 mL). To this solution was added benzylamine (2.18 g, 20.3 mmol) and the mixture was refluxed for 12h. The solvent was removed to give a yellow viscous liquid, which was precipitated into

anhydrous hexanes to afford an off-white solid (4.56 g, 88% yield), mp 105–107°C. ¹H NMR (400 MHz, chloroform-*d*, 22°C): δ=1.34 (8H, s), 1.46 (4H, m), 1.79 (4H, m), 3.99 (4H, t, *J* = 6.4 Hz), 4.79 (4H, s), 6.92 (4H, d, *J* = 8.8 Hz), 7.24-7.34 (10H, m), 7.72 (4H, d, *J* = 8.8 Hz), and 8.31 (2H, s). LRFAB: *m/z* = 561.5 [*M*+H]⁺. HRFAB: calcd for [*M*+H]⁺ C₃₈H₄₄N₂O₂ 561.3481, found 561.3474. Anal. Calcd for C₃₈H₄₄N₂O₂: C, 81.39; H, 7.91, found: C, 81.28; H, 7.86.

6. To a two necked round bottom flask equipped with a magnetic stirrer, condenser, and N₂ inlet were added **5** (3.34 g, 5.96 mmol) and MeOH (130 mL). To this solution were added small portions of NaBH₄ (0.45 g, 11.9 mmol) and the mixture was brought to a gentle reflux and stirred for 12hrs. The solvent was removed to afford a white solid, which was suspended in H₂O and neutralized with 2M HCl. The product was extracted with CHCl₃, the organic layers were combined, dried over MgSO₄, and concentrated to give an off-white solid (3.12 g, 93% yield), mp 64–66°C. ¹H NMR (400 MHz, chloroform-*d*, 22°C): δ=1.34 (8H, s), 1.46 (4H, m), 1.78 (4H, m), 3.75 (4H, s), 3.80 (4H, s), 3.95 (4H, t, *J* = 6.4 Hz), 6.86 (4H, d, *J* = 8.8 Hz), 7.25 (4H, d, *J* = 8.8 Hz), and 7.26-7.34 (10H, m). LRFAB: *m/z* = 565.5 [*M*+H]⁺. HRFAB: calcd for [*M*+H]⁺ C₃₈H₄₈N₂O₂ 565.3794, found 565.3790. Anal. Calcd for C₃₈H₄₈N₂O₂: C, 80.81; H, 8.57, found: C, 80.68; H, 8.47.

7. To a one neck round bottom flask equipped with a magnetic stirrer were added **6** (2.20 g, 3.90 mmol) and MeOH (50 mL). To this solution was added 2M HCl (20 mL) and the mixture was stirred for 1 h. The solvent was removed to give an off-white solid, which was then suspended in acetone and aq. NH₄PF₆ was added until complete dissolution occurred. The solvent was evaporated and the resulting solid was washed thoroughly with H₂O to afford an off-white solid (2.90 g, 87% yield), mp decomp. 150°C. ¹H NMR (400 MHz, acetone-*d*₆, 22°C): δ=1.34 (8H, s), 1.45 (4H, m), 1.76 (4H, m), 4.01 (4H, t, *J* = 6.4 Hz), 4.58 (4H, s), 4.61 (4H, s), 6.99 (4H, d, *J* = 8.8 Hz), 7.45-7.58 (10H, m), and 7.50 (4H, d, *J* = 8.8 Hz). LRFAB: *m/z* = 711.6 [*M*-PF₆]⁺. HRFAB: calcd for [*M*-PF₆]⁺

C₃₈H₅₀N₂O₂PF₆ 711.3514, found 711.3528. Anal. Calcd for C₃₈H₅₀N₂O₂P₂F₁₂: C, 53.27; H, 5.88, found: C, 53.17; H, 5.81.

5.5. References

- 1)Lehn, J.-M. *Supramolecular Chemistry Concepts and Perspectives*; VCH: New York, 1995.
- 2)Lehn, J.-M. *Makromol. Chem., Macromol. Symp.* **1993**, *69*, 1-17.
- 3)Lehn, J.-M. *Angew. Chem. Int. Ed. Engl.* **1990**, *29*, 1304-1319.
- 4)Wilson, L. M. *Macromolecules* **1994**, *27*, 6683-6686.
- 5)Hilger, C.; Dräger, M.; Stadler, R. *Macromolecules* **1992**, *25*, 2498-2501.
- 6)St. Pourcain, C. B.; Griffin, A. C. *Macromolecules* **1995**, *28*, 4116.
- 7)Ducharme, Y.; Wuest, J. D. *J. Org. Chem.* **1988**, *53*, 5787-5789.
- 8)Castellano, R. K.; Rebek, J., Jr. *J. Am. Chem. Soc.* **1998**, *120*, 3657-3663.
- 9)Schubert, U. S.; Widel, C. H.; Eschbaumer, C. *Am. Chem. Soc. Polym. Mat. Sci. Eng.* **1999**, *80*, 22-23.
- 10)Folmer, B. J. B.; Cavini, E.; Sijbesma, R. P.; Meijer, E. W. *J. Chem. Soc., Chem. Commun.* **1998**, 1847-1848.
- 11)Beijer, F. H.; Kooijman, H.; Spek, A. L.; Sijbesma, R. P.; Meijer, E. W. *Angew. Chem. Int. Ed.* **1998**, *37*, 75-77.
- 12)Sijbesma, R. P.; Beijer, F. H.; Brunsveld, L.; Folmer, B. J. B.; Hirschberg, J. J. K. K.; Lange, R. F. M.; Lowe, J. K. L.; Meijer, E. W. *Science* **1997**, *278*, 1601-1604.
- 13)Hirschberg, J. H. K. K.; Beijer, F. H.; van Aert, H. A.; Magusin, P. C. M. M.; Rint P. Sijbesma, R. P.; Meijer, E. W. *Macromolecules* **1999**, *32*, 2696 -2705.
- 14)Ashton, P. R.; Campbell, P. J.; Chrystal, E. J. T.; Glink, P. T.; Menzer, S.; Philp, D.; Spencer, N.; Stoddart, J. F.; Tasker, P. A.; Williams, D. J. *Angew. Chem. Int. Ed. Engl.* **1995**, *34*, 1865-1869.
- 15)Ashton, P. R.; Chrystal, E. J. T.; Glink, P. T.; Menzer, S.; Schiavo, C.; Spencer, N.; Stoddart, J. F.; Tasker, P. A.; White, A. J. P.; Williams, D. J. *Chem. Eur. J.* **1996**, *2*, 709-728.

- 16) Odian, G. *Principles of Polymerization*; Third Edition ed.; John Wiley & Sons, Inc.: New York, 1991.
- 17) Hamilton, S. C.; Semlyen, J. A. *Polymer* **1997**, *38*, 1685-1691.
- 18) Ashton, P. R.; Baxter, I.; Cantrill, S. J.; Fyfe, M. C. T.; Glink, P. T.; Stoddart, J. F.; White, A. J. P.; Williams, D. J. *Angew. Chem. Int. Ed.* **1998**, *37*, 1294-1297.
- 19) Allcock, H. R.; Lampe, F. W. *Contemporary Polymer Chemistry*; Second Edition ed.; Prentice-Hall: New Jersey, 1990.
- 20) van Nostrum, C. F.; Picken, S. J.; Schouten, A.-J.; Nolte, R. J. M. *J. Am. Chem. Soc.* **1995**, *117*, 9957-9965.
- 21) Kimizuka, N.; Fujikawa, S.; Kuwahara, H.; Kunitake, T.; Marsh, A.; Lehn, J.-M. *J. Chem. Soc., Chem. Commun.* **1995**, 2103-2104.
- 22) de Loos, M.; van Esch, J.; Stokroos, I.; Kellogg, R. M.; Feringa, B. L. *J. Am. Chem. Soc.* **1997**, *119*, 12675-12676.
- 23) Guilani, B.; Rasco, M. L.; Hermann, C. F. K.; Gibson, H. W. *J. Heterocyclic Chem.* **1990**, *27*, 1007-1009.
- 24) Montage, M. W. *J. Pharm. Pharmacol.* **1952**, *4*, 533-538.